

PDF hosted at the Radboud Repository of the Radboud University Nijmegen

The following full text is a preprint version which may differ from the publisher's version.

For additional information about this publication click this link.

<http://hdl.handle.net/2066/104018>

Please be advised that this information was generated on 2020-09-19 and may be subject to change.

Aubry transition studied by direct evaluation of the modulation functions of infinite incommensurate systems

T.S. VAN ERP¹ (*) and A. FASOLINO²

¹ *Department of Chemical Engineering - Universiteit van Amsterdam, Nieuwe Achtergracht 166, 1018 WV Amsterdam, The Netherlands*

² *Institute for Theoretical Physics, NSRIM - University of Nijmegen, Toernooiveld 1 - 6525 ED Nijmegen, The Netherlands*

PACS. 05.45.-a – Nonlinear dynamics and nonlinear dynamical systems.

PACS. 61.44.Fw – Incommensurate crystals.

PACS. 64.70.Rh – Commensurate-incommensurate transitions.

Abstract. – Incommensurate structures can be described by the Frenkel Kontorova model. Aubry has shown that, at a critical value K_c of the coupling of the harmonic chain to an incommensurate periodic potential, the system displays the analyticity breaking transition between a sliding and pinned state. The ground state equations coincide with the standard map in non-linear dynamics, with smooth or chaotic orbits below and above K_c respectively. For the standard map, Greene and MacKay have calculated the value $K_c=.971635$. Conversely, evaluations based on the analyticity breaking of the modulation function have been performed for high commensurate approximants. Here we show how the modulation function of the infinite system can be calculated without using approximants but by Taylor expansions of increasing order. This approach leads to a value $K'_c=.97978$, implying the existence of a golden invariant circle up to $K'_c > K_c$.

Introduction. – The Aubry transition in the Frenkel Kontorova model is considered equivalent to the breakup of tori in the standard map [1]. Based on Greene's hypothesis that dissolution of invariant tori can be associated with the sudden change from stability to instability of nearly closed orbits, an accurate evaluation of the critical coupling K_c has been derived [2,3]. Besides, by a rigorous computer proof [4] an upper limit $K_c < 63/64$ has been established above which no golden invariant circles can exist. Here we give a comparably accurate estimate of K_c based on the analyticity breaking of the modulation function. Our approach does not make use of finite commensurate approximants, but of Taylor expansions up to very high order of the modulation function of infinite systems. The fact that the two values of K_c do not coincide seems to imply violation of Greene's assumption.

(*) E-mail:tsvanerp@science.uva.nl

The model. – The Frenkel Kontorova model (FKM) consists of a harmonic chain of atoms interacting with a potential V of period incommensurate to the average lattice spacing l . The total potential energy reads:

$$E = \sum_{i=1}^N \frac{1}{2} (x_i - x_{i-1} - l)^2 + V(x_i) \quad (1)$$

$$\text{with } V(x) = \frac{K}{(2\pi)^2} (1 - \cos(2\pi x)) \quad (2)$$

where x_i is the coordinate of particle i . The usual choice is to set the period of the potential to unity and the average spacing to the golden mean $l = \tau_g = (\sqrt{5} - 1)/2$.

The ground state positions x_i^G can be described by the modulation function g : $x_i^G = il + g(il)$ where $g(x)$ is periodic with the period 1 of the modulation potential.

Correspondence with the standard map. – At equilibrium, the force on each particle has to vanish. The relation $\frac{\partial E}{\partial x_i} = 2x_i - x_{i-1} - x_{i+1} + V'(x_i) = 0$ yields the standard map.

$$\begin{pmatrix} x_{i+1} \\ x_i \end{pmatrix} = \mathbb{T} \begin{pmatrix} x_i \\ x_{i-1} \end{pmatrix} = \begin{pmatrix} 2x_i + V'(x_i) - x_{i-1} \\ x_i \end{pmatrix} \quad (3)$$

Starting from a point (x_1, x_0) , this relation defines iteratively a sequence of points on a torus $(x_{i+1}, x_i) \bmod \mathbb{Z}^2$. For $K < K_c$ subsequent points lie on smooth orbits whereas for $K > K_c$ all orbits become chaotic [5, 6]. The theoretical explanation of this transition follows from the Kolmogorov, Arnold and Moser (KAM) theorem [7].

The standard map and the Aubry transition can be related by considering the trajectories with an infinitesimal change in starting point and their relation to the sliding phonon mode in FKM. A small change of starting point $(\delta x_1, \delta x_0)$ will lead to successive changes from the original trajectory of eq. (3), which up to first order in $\delta \mathbf{x}$ are:

$$\begin{pmatrix} \delta x_{i+1} \\ \delta x_i \end{pmatrix} = \begin{pmatrix} 2 + V''(x_i) & -1 \\ 1 & 0 \end{pmatrix} \begin{pmatrix} \delta x_i \\ \delta x_{i-1} \end{pmatrix} \quad (4)$$

The time dependence of phonon eigenvectors ϵ of the FKM, $\epsilon_i = x_i(t) - x_i^G \sim e^{i\omega t}$, satisfy:

$$\epsilon_{i+1} = 2\epsilon_i - \epsilon_{i-1} + (V''(x_i) - \omega^2)\epsilon_i \quad (5)$$

When $\omega = 0$, eq. (5) for ϵ_i becomes equivalent to eq. (4) for δx_i . If the standard map trajectories are unstable with respect to initial conditions, the divergence of $\delta \mathbf{x}$ would imply localization of the sliding mode if $\omega = 0$ belongs to the spectrum [5]. Since for $\omega = 0$, $\epsilon_i = 1 + g'(il)$ one can easily imagine that an exponentially localized eigenvector yields a discontinuous modulation function g . This in turn leads to pinning of the FKM and to the disappearance of the sliding mode. Interestingly we have noted [8] that in the neighborhood of K_c a tendency to localization of the lowest frequency mode occurs, showing up in a drop of the participation ratio. We have conjectured that localization of the zero-frequency mode is the precursor of the structural transition which leads to the opening of the phonon gap.

The critical value K_c has been determined to a high precision as $K_c = 0.971635406$ by MacKay by renormalization of invariant circles within Greene's hypothesis [3]. In this paper, we propose a route to the calculation of K_c which does not need this hypothesis.

Modulation functions at the Aubry transition. – Aubry has discussed the analyticity breaking transition also by applying a perturbative approach to the equilibrium equation for the modulation function.

$$2g(x) - g(x+l) + g(x-l) = -V'(x+g(x)) \quad (6)$$

The KAM theorem could be applied to prove that there exists a continuous function, which obeys eq. (6), when the potential is smooth enough and K is small. We follow the empirical approach of ref. [9], which gives insight in the small denominator problem. By writing V' in Fourier series as

$$V'(x) = K \sum_{m=-\infty}^{+\infty} V_m e^{2\pi i m x} \quad (7)$$

and approximating $V'(x+g(x)) \approx V'(x)$ in eq. (6) we find the modulation function to be:

$$g(x) = -K \sum_m \frac{V_m}{\omega_m^2} e^{2\pi i m x} \quad (8)$$

with $\omega_m = 2|\sin(\pi m l)|$. Notice that this approach applies to a general periodic potential V . The denominators ω_m^2 can become infinitesimally small, especially for Fibonacci numbers F_n ($F_0 = F_1 = 1, F_i = F_{i-1} + F_{i-2}$). With the relation $F_{n-1} - F_n \tau_g = (-\tau_g)^{n+1}$ the divergence of the denominators are:

$$\lim_{n \rightarrow \infty} \frac{1}{\omega_{F_n}^2} = \frac{1}{4\pi^2} \left(\frac{1}{\tau_g^2} \right)^{n+1} \quad (9)$$

For sufficiently small values of K , this divergence is limited. Aubry [9] gave, with a simple derivation, an upper bound for K above which an analytical modulation function can no longer exist. This value for potential (2) is 4π , which is much larger than the actual K_c . Our goal is to find the value of K for which divergence of the denominators really takes place and compare this value with the one obtained by MacKay [3]. The equivalence of these two approaches relies on the validity of Greene's hypothesis.

Approximations of the modulation function of infinite systems and evaluation of K_c . – We rewrite eq. (6) with potential (2) by applying the discrete Fourier transform:

$$g(x) = \sum_{k=-\infty}^{+\infty} X_k e^{2\pi i k x} \quad \text{with inverse:} \quad X_k = \int_0^1 dx g(x) e^{-2\pi i k x} \quad (10)$$

yielding:

$$\omega_k^2 X_k = \frac{K i}{4\pi} \int_0^1 dx e^{-2\pi i k x} \left[e^{2\pi i x} e^{2\pi i g(x)} - e^{-2\pi i x} e^{-2\pi i g(x)} \right] \quad (11)$$

By expanding $\exp(2\pi i g(x))$ as in [10] eq. (11) becomes:

$$\omega_k^2 X_k = \frac{K i}{4\pi} \sum_{m=0}^{\infty} \frac{(i 2\pi)^m}{m!} \sum_{k_1 k_2 \dots k_m} \left[X_{k_1} X_{k_2} \dots X_{k_m} \delta_{k_1+k_2+\dots+k_m+1,k} \right. \\ \left. - (-1)^m X_{k_1} X_{k_2} \dots X_{k_m} \delta_{k_1+k_2+\dots+k_m-1,k} \right] \quad (12)$$

To transform eq. (12) into an expansion in K we define:

$$X_k = KX_k^1 + K^2X_k^2 + K^3X_k^3 + \dots \quad (13)$$

yielding:

$$\begin{aligned} \omega_k^2 X_k^n = & \frac{i}{4\pi} [\delta_{1,k} - \delta_{-1,k}] \delta_{1,n} + \frac{i}{4\pi} \sum_{m=1}^{\infty} \frac{(i2\pi)^m}{m!} \sum_{n_1 n_2 \dots n_m} \sum_{k_1 k_2 \dots k_m} \delta_{n_1+n_2+\dots+n_m+1,n} \\ & \left[X_{k_1}^{n_1} X_{k_2}^{n_2} \dots X_{k_m}^{n_m} \delta_{k_1+k_2+\dots+k_m+1,k} - (-1)^m X_{k_1}^{n_1} X_{k_2}^{n_2} \dots X_{k_m}^{n_m} \delta_{k_1+k_2+\dots+k_m-1,k} \right] \quad (14) \end{aligned}$$

Eq. 14 could have been obtained directly by applying to both sides of eq. (6) the operator $D \equiv \frac{1}{n!} \frac{d^n}{dK^n} \int_0^1 dx e^{-2\pi i k x} \dots |_{K=0}$. From eq. (14) it is straightforward to obtain first order approximation $g(x) = -\frac{K}{2\pi} \frac{\sin(2\pi x)}{\omega_1^2} + \mathcal{O}(K^2)$. Since higher harmonics X_k scale with K^k [10] $X_k^n = 0$ for $|k| > n$. A manageable iterative algorithm to calculate the coefficients X_k^n from those of lower order can be derived by defining the matrix $P(n, k, m)$ as:

$$P(n, k, m) = \frac{(2\pi i)^m}{m!} \sum_{n_1 n_2 \dots n_m} \sum_{k_1 k_2 \dots k_m} X_{k_1}^{n_1} X_{k_2}^{n_2} \dots X_{k_m}^{n_m} \delta_{n_1+n_2+\dots+n_m, n} \delta_{k_1+k_2+\dots+k_m, k} \quad (15)$$

$P(n, k, m) = 0$ for $|k| > n$ and for $m > n$. Eventually we are only interested in the elements with $m = 1$ which give the Taylor-Fourier coefficients of the modulation function

$$X_k^n = \frac{P(n, k, 1)}{2\pi i} \quad (16)$$

However elements of P with $m > 1$ are used during the calculation, allowing an effective iterative procedure. To this purpose we rewrite eq. (15) for $m > 1$ as:

$$\begin{aligned} P(n, k, m) = & \frac{2\pi i}{m} \sum_{n_m} \sum_{k_m} X_{k_m}^{n_m} \frac{(2\pi i)^{m-1}}{(m-1)!} \sum_{n_1 n_2 \dots n_{m-1}} \sum_{k_1 k_2 \dots k_{m-1}} \\ & \left[X_{k_1}^{n_1} X_{k_2}^{n_2} \dots X_{k_{m-1}}^{n_{m-1}} \delta_{n_1+n_2+\dots+n_{m-1}, n-n_m} \delta_{k_1+k_2+\dots+k_{m-1}, k-k_m} \right] \quad (17) \end{aligned}$$

This leads to our final recursive relations:

$$\begin{aligned} P(1, \pm 1, 1) &= \frac{\mp 1}{2\omega_1^2} \\ P(n, k, 1) &= -\frac{1}{2} \omega_k^{-2} \sum_{m=1}^{n-1} \left[P(n-1, k-1, m) - (-1)^m P(n-1, k+1, m) \right] \quad (18) \\ P(n, k, m) &= \frac{1}{m} \sum_{n'=1}^{n-m+1} \sum_{k'=\max\{-n', k-n+n'\}}^{\min\{n', k+n-n'\}} P(n', k', 1) P(n-n', k-k', m-1), \quad (n \geq m > 1) \end{aligned}$$

The second relation is nothing but eq. (14) written in term of P for $m = 1$; The first one starts the iteration for $n = 1$. The third relation uses eq. (17) to calculate elements with $m > 1$. All elements of $P(n, k, m)$ are real and the set of equations (18) is very efficient for

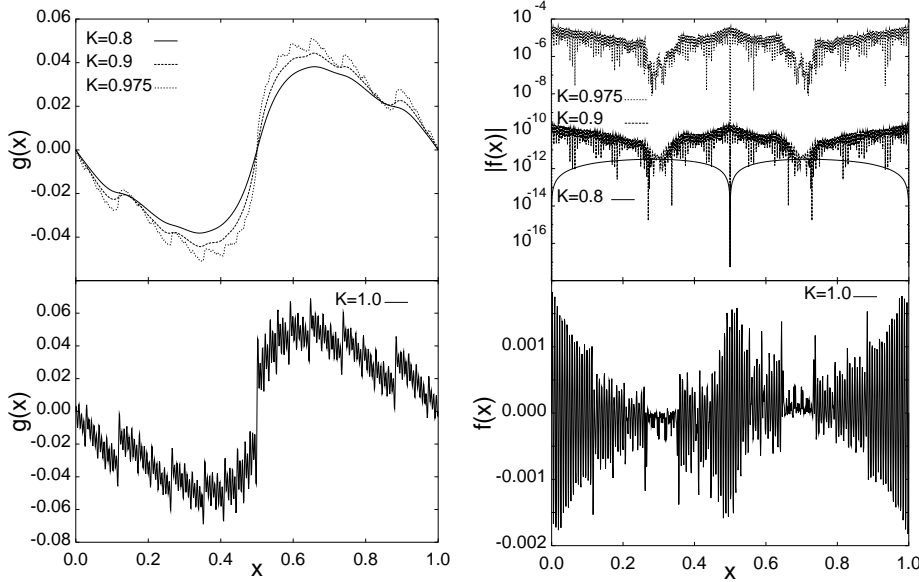


Fig. 1 – Left: $n = 150$ -th order modulation functions, right: resulting forces for the FKM. Top: $K = 0.8, 0.9$ and 0.975 , bottom: $K = 1.0$

numerical calculations. Memory is the bottleneck at very high Taylor order, since the number of nonzero elements up to order n , which have to be stored, increases as $\sim n^3$. CPU time also increases with n^3 but remains moderate, a 150-th order calculation taking about 15 minutes on a Pentium.

The iterative calculation of eq. (18) has to be performed only once to get, by use of eq. (16), (13) and (10), all modulation functions of order n for $K \in [0 : K_c]$. For $K > K_c$ we expect this method to break up either because eq. (13) is no longer converging for some k or because infinite high-frequency oscillations appear in the discrete Fourier sum.

In fig. 1 we plot the modulation functions for different K , together with the forces $f(x) \equiv 2g(x) - g(x-l) - g(x+l) + V'(x+g(x))$, which should vanish for the exact modulation function. The appearance of high frequency oscillations at $K = 1 > K_c$ is clearly visible, yielding non-vanishing forces. In fig. 2 we show the Fourier coefficients X_k up to Taylor order $n = 150$ for several values of K across the transition. Their values agree with numerical evaluations on commensurate approximants [11]. The behaviour as K^k expected for $K \rightarrow 0$ is still a good representation even at $K = 0.5 \sim K_c/2$. This behaviour is found for all k and is not limited to $k \lesssim 20$ by numerical accuracy as found in [11].

Inspection of the modulation function as given in fig. 1 is not enough to pinpoint K_c . However the behaviour with increasing n of the coefficients X_k^n can lead to a precise evaluation based on the following reasoning. By assuming that the Taylor-Fourier coefficients grow with a power law:

$$\begin{aligned} X_k^n &\sim P(n, k, 1) \sim (\lambda_k)^n \\ X_n^n &\sim P(n, n, 1) \sim (\lambda_n)^n \end{aligned} \quad (19)$$

both $K^n X_n^n$ and the sum (13) remain convergent up to $K\lambda < 1$ whence we can estimate K_c

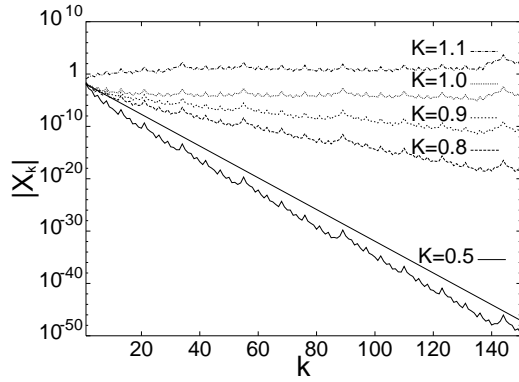


Fig. 2

Fig. 2 – $|X_k|$ as function of k for $n = 150$ and several values of K for the FKM. The expected behavior given by K^k is also given for $K = 0.5$.

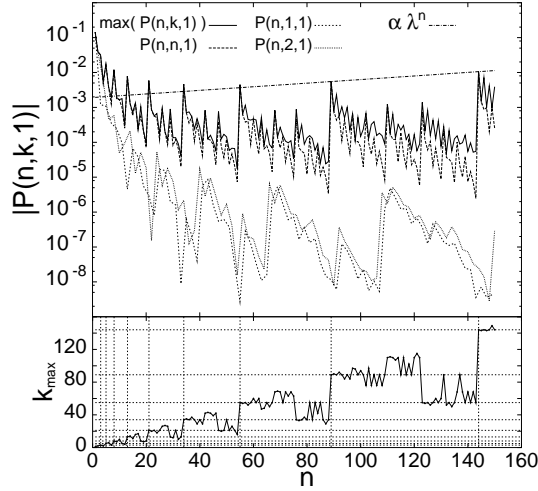


Fig. 3

Fig. 3 – $|P(n, k, 1)|$ as function of n for different k for the FKM. The plotted curves are $\max(|P(n, k, 1)|)$ (the k_{max} value of k corresponding to this maximum is given in the lower panel), $|P(n, n, 1)|$, $|P(n, 1, 1)|$ and $|P(n, 2, 1)|$. Note that when n is a Fibonacci number, the maximum is always at $k = n$. The straight line is the fit $y = \alpha \lambda^n$ through $P(89, 89, 1)$ and $P(144, 144, 1)$, giving $\lambda = 1.012 \Rightarrow K_c(F_{11}) \sim 0.988$. Dotted lines in the lower panel correspond to the Fibonacci numbers.

as:

$$K_c = \frac{1}{\max\{\lambda_k, \lambda_n\}} \quad (20)$$

In fig. 3 we show the elements $|P(n, k, 1)|$ as function of n for several values of k . We also show $\max(|P(n, k, 1)|)$, i.e. the maximum of $|P(n, k, 1)|$ for each n . The k -value corresponding to this maximum, indicated as k_{max} , is shown in the lower panel. In particular for n corresponding to Fibonacci numbers (34, 55, 89, 144), k_{max} is equal to n . Moreover, at these values of n we see sudden jumps due to the fact that ω_k^{-2} diverges like eq. (9). Besides, a power law dependence of the maxima at Fibonacci numbers begins to develop for large n as indicated by the straight line.

From these numerical calculations we can conclude that λ_n is the dominant exponent. Therefore for the calculation of K_c we need to calculate eq. 18 only for $k = n$ where it takes a simpler form

$$P(n, n, 1) = -\frac{1}{2} \omega_k^{-2} \sum_{m=1}^{n-1} P(n-1, n-1, m) \quad (21)$$

$$P(n, n, m) = \frac{1}{m} \sum_{n'=1}^{n-m+1} P(n', n', 1) P(n-n', n-n', m-1), \quad (n \geq m > 1) \quad (22)$$

For this case only $\frac{1}{2}n(n+1)$ elements have to be stored, and calculations up to the order n of a few thousands can easily be achieved in order to get a good estimate of λ_n . In fig. 4 a)

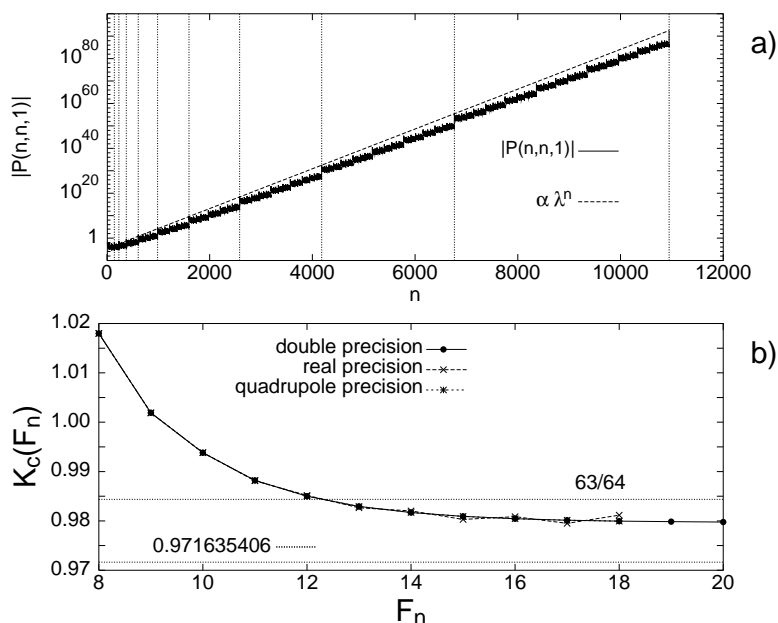


Fig. 4 – a): $|P(n, n, 1)|$ as a function of n . Vertical lines indicate the Fibonacci numbers. The calculation is up to order $n = F_{20} = 10946$. The line $\alpha \lambda^n$ corresponds to the best fit through $n = F_{20} = 10946$ and $n = F_{19} = 6765$. $1/\lambda$ corresponds to 0.979778542 , which is our best approximation of K_c . b): $K_c(F_n)$ approximation from eq. 23 as a function of F_n . Note that the order is up to $F_{20} = 10946$. The horizontal dotted lines are the upper limit $63/64$ [4] and MacKay’s value [3]. For examination of floating point errors also real and quadruple precision are included up to F_{18} . Only real precision gives an appreciable difference, but not systematic.

$P(n, n, 1)$ is calculated up to $n = F_{20}$ and found to have a power-law behaviour. As we assume that $P(F_n, F_n, 1) \sim (\frac{1}{K_c})^{F_n}$, we can define successive approximations of K_c as:

$$K_c(F_n) = \left| \frac{P(F_n, F_n, 1)}{P(F_{n-1}, F_{n-1}, 1)} \right|^{\frac{1}{F_n - 2}} \quad (23)$$

In fig. 4 b) we show $K_c(F_n)$ up to order $F_{20} = 10946$, with $K_c(F_{20}) = 0.979778542$, which is close but significantly different than MacKay’s value $K_c = 0.971635406$ [3]. The value of $K_c = 0.979 < 63/64$ determined by our procedure seems well converged and is unlikely to reach MacKay’s value for higher F_n . We have also checked that quadruple precision does not change our numerical results. The discrepancy between our value of K_c , which is directly related to non analyticity of the modulation function, and that of the transition to instability in the standard map questions the validity of Greene’s hypothesis.

REFERENCES

- [1] FLORIA, L. M. and MAZO, J. J., *Adv. Phys.*, **45** (1996) 505
- [2] GREENE, J. M., *J. Math. Phys.*, **20** (1979) 1183
- [3] MACKAY, R. S., *Renormalisation in area preserving maps*, *Ph.D. thesis* (Princeton (Univ. Microfilms Int., Ann Arbor, Michigan)) 1982
- [4] MACKAY R.S. and PERCIVAL, I.C., *Commun. Math. Phys.*, **98** (1985) 469

- [5] AUBRY S., *Physica*, **7D** (1983) 240
- [6] CHIRIKOV B. V., *Phys. Rep.*, **52** (1979) 263
- [7] TABOR, M., *Chaos and Integrability in Nonlinear Dynamics: An Introduction*, (Wiley, New York) 1989, p. 105.
- [8] VAN ERP, T. S. and FASOLINO, A. and RADULESCU, O. and JANSSEN, T., *Phys. Rev. B*, **60** (1999) 6522
- [9] AUBRY S. and ANDRÉ G., *Ann. Isr. Phys. Soc.*, **3** (1980) 133 reprinted in *The Physics of Quasi-Crystals*, edited by P.J. Steinhard and S. Oslund (World Scientific, Singapore, 1987), pp 554-595.
- [10] CONSOLI L., KNOPS H. and FASOLINO A., *Phys. Rev. Lett.*, **85** (2000) 302
- [11] CONSOLI L., KNOPS H. and FASOLINO A., *Phys. Rev. E*, **64** (2001) 016601